

# Ni/Li Disordering in Layered Transition Metal Oxide: Electrochemical Impact, Origin, and Control

Jiaxin Zheng,<sup>†</sup> Yaokun Ye,<sup>†</sup> Tongchao Liu,<sup>†</sup> Yinguo Xiao,<sup>†</sup> Chongmin Wang,<sup>‡,§</sup> Feng Wang,<sup>§,§</sup> and Feng Pan<sup>\*,†,§</sup>

<sup>†</sup>School of Advanced Materials, Shenzhen Graduate School, Peking University, Shenzhen 518055, People's Republic of China

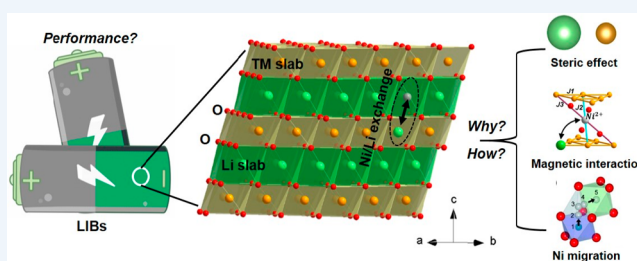
<sup>‡</sup>Environmental Molecular Sciences Laboratory, Pacific Northwest National Laboratory, 902 Battelle Boulevard, Richland, Washington 99352, United States

<sup>§</sup>Sustainable Energy Technologies Department, Brookhaven National Laboratory, Upton, New York 11973, United States

**CONSPECTUS:** Lithium ion batteries (LIBs) not only power most of today's hybrid electric vehicles (HEV) and electric vehicles (EV) but also are considered as a promising system for grid-level storage. Large-scale applications for LIBs require substantial improvement in energy density, cost, and lifetime. Layered lithium transition metal (TM) oxides, in particular,  $\text{Li}(\text{Ni}_x\text{Mn}_y\text{Co}_z)\text{O}_2$  (NMC,  $x + y + z = 1$ ) are the most promising candidates as cathode materials with the potential to increase energy densities and lifetime, reduce costs, and improve safety. In order to further boost Li storage capacity, a great deal of attention has been directed toward developing Ni-rich layered TM oxides. However, structural disorder as a result of Ni/Li exchange in octahedral sites becomes a critical issue when Ni content increases to high values, as it leads to a detrimental effect on Li diffusivity, cycling stability, first-cycle efficiency, and overall electrode performance. Increasing effort has been dedicated to improving the electrochemical performance of layered TM oxides via reduction of cationic mixing. Therefore, it is important to summarize this research field and provide in-depth insight into the impact of Ni/Li disordering on electrochemical characteristics in layered TM oxides and its origin to accelerate the future development of layered TM oxides with high performance.

In this Account, we start by introducing the Ni/Li disordering in  $\text{LiNiO}_2$ , the experimental characterization of Ni/Li disordering, and analyzing the impact of Ni/Li disordering on electrochemical characteristics of layered TM oxides. The antisite Ni in the Li layer can limit the rate performance by impeding the Li ion transport. It will also degrade the cycling stability by inducing anisotropic stress in the bulk structure. Nevertheless, the antisite Ni ions do not always bring drawbacks to the electrochemical performance; some studies including our works found that it can improve the thermal stability and the cycling structure stability of Ni-rich NMC materials. We next discuss the driving forces and the kinetic advantages accounting for the Ni/Li exchange and conclude that the steric effect of cation size and the magnetic interactions between TM cations are the two main driving forces to promote the Ni/Li exchange during synthesis and the electrochemical cycling, and the low energy barrier of  $\text{Ni}^{2+}$  migration from the 3a site in the TM layer to the 3b site in the Li layer further provides a kinetic advantage. Based on this understanding, we then review the progress made to control the Ni/Li disordering through three main ways: (i) suppressing the driving force from the steric effect by ion exchange; (ii) tuning the magnetic interaction by cationic substitution; (iii) kinetically controlling Ni migration.

Finally, our brief outlook on the future development of layered TM oxides with controlled Ni/Li disordering is provided. It is believed that this Account will provide significant understanding and inspirations toward developing high-performance layered TM oxide cathodes.



## 1. INTRODUCTION

Layered lithium transition metal (TM) oxides,  $\text{LiTMO}_2$  (TM = Ni, Mn, Co, or  $\text{Ni}_x\text{Mn}_y\text{Co}_z$ ,  $x + y + z = 1$ ), have been extensively studied as important cathode materials for high-energy-density lithium ion batteries (LIBs).<sup>1</sup> They adopt the well-known  $\alpha\text{-NaFeO}_2$  type structure and consist of alternating layers of Li ions and TM ions separated by oxygen atomic layers (Figure 1). Ni/Li exchange (or Ni/Li disordering, wherein Ni occupies 3b sites in the Li layer and Li occupies 3a sites in the TM layer) usually happens between the Li layer

and TM layer in these layered TM oxides (Figure 1), not only during the material synthesis procedure but also during the electrochemical cycling process.<sup>2–10</sup>

Ni/Li disordering, side reactions between the layered TM oxides and the nonaqueous electrolyte, surface crystallographic reconstruction, and cracking of the secondary particle agglomerates account for degradation mechanisms of layered

Received: January 16, 2019

Published: June 10, 2019

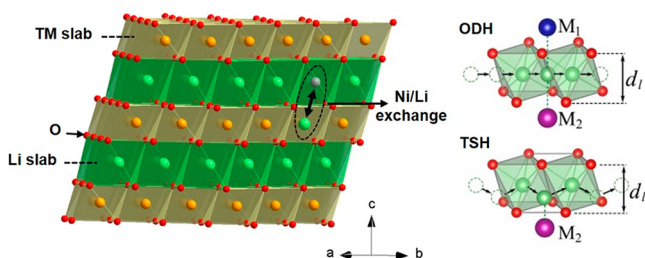


**Figure 1.**  $\alpha$ -NaFeO<sub>2</sub> type structure of layered NMC materials with one pair of Ni/Li exchange (left panel) and illustration of the ODH (oxygen dumbbell hopping) and TSH (tetrahedral site hopping) types of Li ion diffusion pathways (right panel).

TM oxides as cathodes for LIBs.<sup>2–5,11–14</sup> In particular, Ni/Li disordering is not only an intrinsic structure property of layered TM oxides, which affects nearly all the aspects of electrochemical performance (the rate performance, discharge capacity, cycling stability, and thermal stability),<sup>2–5,11,12,15–17</sup> but also closely correlated with surface crystallographic reconstruction and the cracking of the secondary particle agglomerates.<sup>18–20</sup> Especially in Co-free (or low-Co) and Ni-rich layered LiTMO<sub>2</sub>, which has received a great deal of recent attention, Ni/Li disordering becomes so prominent that it is often considered to play a key role in determining the electrochemical performance.<sup>21–25</sup> For example, when the Ni/Li exchange is reduced from 3.2% to 2.6% (only by 0.6%) in LiNi<sub>0.7</sub>Mn<sub>0.15</sub>Co<sub>0.15</sub>O<sub>2</sub>,<sup>21</sup> the discharge capacity is improved from 162 mAh g<sup>-1</sup> to 197 mAh g<sup>-1</sup> at a constant current of 10 mA g<sup>-1</sup>. Hence, many works have attempted to suppress the degree of Ni/Li disordering to improve the performance of layered TM oxides.<sup>3,21,22,24</sup> On the other hand, previous works showed that some degree of disordering can benefit the structural stability during electrochemical cycling<sup>4,26,27</sup> for layered LiTMO<sub>2</sub> at high states of charge and the thermal stability of Ni-rich Li(Ni<sub>x</sub>Mn<sub>y</sub>Co<sub>z</sub>)O<sub>2</sub> (NMC,  $x + y + z = 1$ ).<sup>17</sup> From this aspect, a minimum degree of Ni/Li disordering for Ni-rich NMC is needed to obtain the best electrochemical performance.

In this Account, we will first introduce the Ni/Li disordering in LiNiO<sub>2</sub> and the experimental characterizations, analyze the electrochemical impact of Ni/Li disordering in layered TM oxides, and then discuss the detailed mechanism accounting for the Ni/Li exchange. Finally, the methods to control the degree of Ni/Li disordering in layered TM oxides will be summarized.

## 2. Ni/Li DISORDERING IN LiNiO<sub>2</sub> AND EXPERIMENTAL CHARACTERIZATIONS

Ni/Li disordering was first found in layered LiNiO<sub>2</sub>, which was considered as an alternative to LiCoO<sub>2</sub> because of its lower cost, higher reversible capacity (ca. 200 mAh g<sup>-1</sup>) and better environmental compatibility.<sup>2</sup> As the trivalent oxidation state for Ni is relatively unstable, there are always divalent nickel ions leading to the Li<sub>1–z</sub>Ni<sub>1+z</sub>O<sub>2</sub> formula ( $0.00 < z \leq 0.20$ ).<sup>28</sup> This gives rise to Ni/Li disordering, since the occupation of Ni<sup>2+</sup> in the “interlayer” Li 3b site is more favorable than that of Ni<sup>3+</sup> because of the similar size of Ni<sup>2+</sup> and Li<sup>+</sup> ( $r_{\text{Ni}^{3+}} = 0.56 \text{ \AA}$ ,  $r_{\text{Ni}^{2+}} = 0.69 \text{ \AA}$ ,  $r_{\text{Li}^+} = 0.76 \text{ \AA}$ ). With the further development of Ni/Co and Ni/Mn binary oxides and ternary NMC compounds, the problem of Ni/Li disordering still exists and has attracted sustained research interest.<sup>2,3,5</sup>

X-ray diffraction (XRD) is the most widely used approach for Ni/Li disordering characterization. The ratio of the integrated intensity of  $I(003)/I(104)$  and the merging of the  $(018)_R/(110)_R$  pairs are two key parameters reflecting the degree of the mixing of Ni and Li ions.<sup>15,17</sup> If the integrated intensity of  $I(003)/I(104)$  is  $< 1.2$  and the  $(018)_R/(110)_R$  pairs begin to merge, it means that Ni and Li ion mixing happens. Rietveld refinement of the collected XRD patterns is usually conducted to determine the content of Ni at 3b sites. Neutron powder diffraction is a more powerful technique to determine the content of Ni/Li exchange directly, and the disordered arrangement model can be adopted in the Rietveld refinement.<sup>29</sup> Cationic mixing near the surface of layered LiTMO<sub>2</sub> particles can be observed by bright field transmission electron microscopy (TEM) image and the corresponding electron diffraction patterns, but the content of cationic mixing cannot be determined.<sup>3,30</sup>

## 3. ELECTROCHEMICAL IMPACT OF Ni/Li DISORDERING

### 3.1. Impact on the Rate Performance and Discharge Capacity

Previous studies reported that Ni/Li disordering would impede the kinetic diffusion of Li ion during electrochemical cycling for layered LiTMO<sub>2</sub>, thus affecting the rate capability and discharge capacity. For example, LiNi<sub>0.5</sub>Mn<sub>0.5</sub>O<sub>2</sub> shows surprisingly high capacity (200 mAh g<sup>-1</sup> at C/20) over current electrode materials at low rates (1C rate = 280 mA g<sup>-1</sup>), but this advantage completely disappears at commercially interesting rates (125 mAh g<sup>-1</sup> at 1C),<sup>24</sup> due to the high Ni/Li exchange (about 10%).<sup>25</sup> With the content of Ni/Li exchange decreased to 0.5%, it delivers a discharge capacity of 183 mAh g<sup>-1</sup> even at 6C rate. Zhang et al. reported that in LiNi<sub>1/3</sub>Mn<sub>1/3</sub>Co<sub>1/3</sub>O<sub>2</sub> an increased amount of Ni/Li disordering from 1.26% to 2.93% would lead to the diffusion coefficient of Li ion decreased from  $4.4 \times 10^{-10} \text{ cm}^2/\text{s}$  to  $2.6 \times 10^{-10} \text{ cm}^2/\text{s}$ .<sup>12</sup>

In the layered structure for LiTMO<sub>2</sub>, there are two kinds of Li diffusion pathways (Figure 1):<sup>31</sup> one is that Li ions diffuse from one octahedral site to the next octahedral site by hopping through the oxygen dumbbell directly, and this is named oxygen dumbbell hopping (ODH); the other is that Li ions diffuse from one octahedral site to the next octahedral site by hopping through a divacancy left by Li diffusion to an intermediate tetrahedral site with transition metals around it, and the is named tetrahedral site hopping (TSH). We can see that the activation barriers of both diffusion paths depend on not only the electrostatic interaction between Li ion in the activated state and the TM cations but also the strain effect (the size of the saddle point of the oxygen dumbbell for ODH and the size of the tetrahedral site for TSH), leading to the energy barriers for the ODH path and TSH path ranging from 0.75 to 0.91 eV and from 0.36 to 0.54 eV,<sup>31</sup> respectively.

The site-exchanged Ni ions within the Li slabs always show Ni<sup>2+</sup> state.<sup>32</sup> The antisite Ni<sup>2+</sup> impedes the kinetics of Li diffusion in the following ways: (i) Because the Li ion migration in layered LiTMO<sub>2</sub> is a 2D diffusion and the pathway is within the Li ion layer, the antisite Ni<sup>2+</sup> would disrupt the Li ion diffusion path.<sup>31</sup> (ii) The higher charge of antisite Ni should lead to a stronger electrostatic repulsion of the migrating Li ions, resulting in a lower Li mobility. (iii) As described above, the activation energy of both ODH and TSH

diffusion is closely associated with the strain effect, which is determined by the *c*-lattice parameter (Li slab space). Due to the stronger interaction of O–Ni<sup>2+</sup>–O than that of O–Li<sup>+</sup>–O, the antisite Ni<sup>2+</sup> will reduce the Li slab space, resulting in a higher activation barrier to lithium diffusion.<sup>33</sup> According to the work by Kang et al., the Li slab space reduces from 2.64 to 2.62 Å when 8.3% of Ni/Li exchange happens in LiNi<sub>0.5</sub>Mn<sub>0.5</sub>O<sub>2</sub>, and this very small change (~0.02 Å) results in a 20–30 meV increase in the activation barrier for the TSH route<sup>24</sup> (Figure 2). (iv) During the first charge, the Ni<sup>2+</sup> ions at

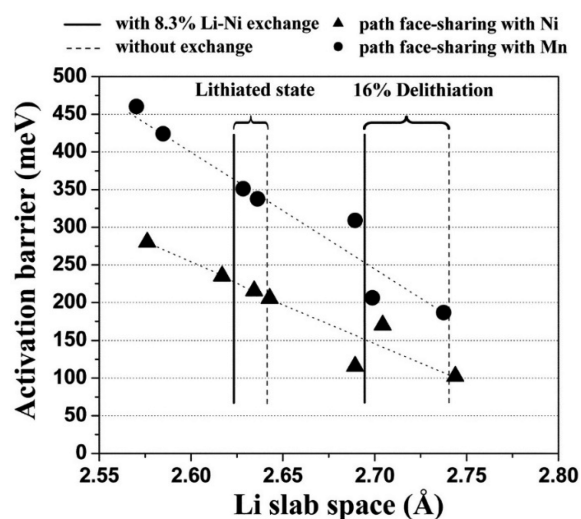


**Figure 2.** Calculated activation barrier for Li migration in Li(Ni<sub>0.5</sub>Mn<sub>0.5</sub>)O<sub>2</sub> with 8.3% Ni/Li exchange as a function of the Li slab space. Adapted with permission from ref 24. Copyright 2006 AAAS.

Li sites are oxidized to smaller Ni<sup>3+</sup> ions. This causes a local shrinkage around those Ni ions, and therefore it is difficult to insert lithium ions back into the positions around them,<sup>34,35</sup> which is responsible for first-cycle irreversibility.

### 3.2. Impact on the Cycling Stability

It was also reported that the Ni/Li disordering affects the structure stability and the phase transformation during electrochemical cycling in layered LiTMO<sub>2</sub>.<sup>2,20,36</sup> For example, in LiNi<sub>1/3</sub>Mn<sub>1/3</sub>Co<sub>1/3</sub>O<sub>2</sub>, the reversible capacity retention can be well-maintained as high as 90.3% after 50 cycles at 0.1C for the sample with Ni/Li disordering of 1.9%, while it is only 50.1% for the sample with Ni/Li disordering of 4.3%.<sup>37</sup> The microscopic mechanisms can be explained in the following ways: (i) When Ni ions with valence state of 2+, 3+, and 4+ are replaced with Li<sup>+</sup>, the local Coulombic interaction of the related TM ions is changed, and the network of superexchange interactions<sup>20,32,38,39</sup> among the TM ions is also broken due to lack of localized d-orbital electrons on the antisite Li ions. Thus, both the Coulombic interaction and superexchange interaction will give rise to the distortion force and lead to the anisotropic stress in the bulk structure. Using ab initio calculations, Yu et al. found a large anisotropic stress of the unit cell in LiNi<sub>0.42</sub>Mn<sub>0.42</sub>Co<sub>0.16</sub>O<sub>2</sub> with Ni/Li disordering, and it increases sharply with the increasing Ni/Li disordering, especially during the delithiation process<sup>20</sup> (Figure 3). The anisotropic stress can be reflected in experiments by pronounced changes in the *c/a*-ratio determined by XRD measurement and may result in irreversible crystal structure

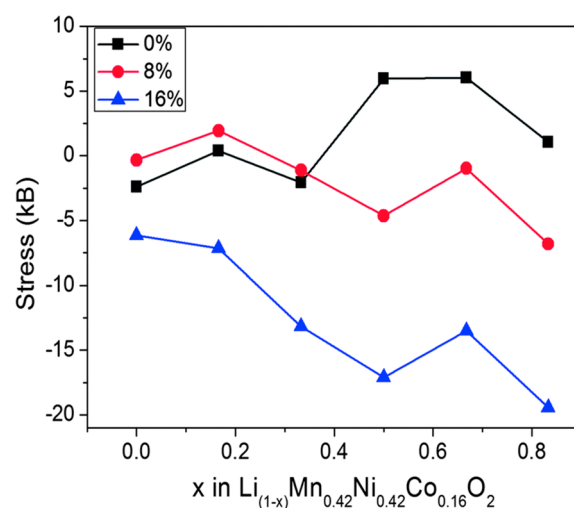


**Figure 3.** Calculated stress of the unit cell with different contents of Ni/Li exchange in layered Li<sub>(1-x)</sub>Mn<sub>0.42</sub>Ni<sub>0.42</sub>Co<sub>0.16</sub>O<sub>2</sub>. Adapted with permission from ref 20. Copyright 2014 Royal Society of Chemistry.

transformation and even cause cracks in the electrode particles.<sup>40</sup> (ii) During electrochemical cycling, the antisite Ni ions would gradually migrate to the particle surface due to the low energy barrier for Ni<sup>2+</sup> migration (~0.25 eV), leading to Ni depletion in the bulk, structural instability, and consequently cathode voltage and capacity fade.<sup>18,19</sup>

On the other hand, other studies reported that high delithiation of layered LiTMO<sub>2</sub> leads to a very unstable situation since the lithium layers become increasingly more depleted to lead to the expansion of Li slab space. The Ni/Li disordering can mitigate the slab-distance contraction at high states of charge, stabilize the structure, and prevent collapse, thus benefiting the structural stability during electrochemical cycling.<sup>4,26,27</sup> For example, Sun et al. reported that in LiNi<sub>1/3</sub>Mn<sub>1/3</sub>Co<sub>1/3</sub>O<sub>2</sub>, though the sample with 2.14% of Ni/Li disordering shows better rate performance than the sample with 5.61% of Ni/Li disordering, the latter sample shows slower voltage decay and capacity fade during long-term cycling between 4.8 and 2.5 V.<sup>27</sup>

### 3.3. Impact on the Thermal Stability

Interestingly, our recent theoretical work found that Ni/Li disordering would decrease the thermal stability of the “Ni=Mn” group NMC.<sup>17</sup> However, we simultaneously found that Ni/Li disordering would benefit the thermal stability of Ni-rich NMC, which also agrees with previous experimental reports on Ni-rich NMC materials.<sup>15,16</sup> Because the Ni in the Li layer would form 180° Ni–O–Ni superexchange chains in Ni-rich NMC materials, the O ion between the spin parallel Ni forms  $\sigma$ -bonding with one Ni ion and the O ion between the spin antiparallel Ni forms  $\pi$ -bonding. This would enhance the thermal stability for Ni-rich NMC materials.

## 4. THE ORIGIN OF Ni/LI DISORDERING

### 4.1. Steric Effect of Cation Size

Most previous studies attributed the Ni/Li exchange in layered TM oxides to the similar size of Ni<sup>2+</sup> and Li<sup>+</sup>. Figure 4 shows the AMO<sub>2</sub> composition (M = 3d TM); the ordered distribution of A<sup>+</sup> and M<sup>3+</sup> cation in one (111) plane out of two of the rock salt type structure ( $\alpha$ -LiFeO<sub>2</sub>) leads to the formation of the well-known  $\alpha$ -NaFeO<sub>2</sub> type layered

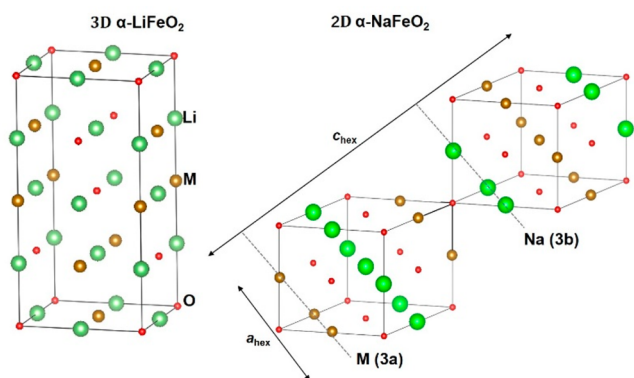


**Figure 4.** Formation of the layered structure by cation ordering within the rock salt structure.

structure.<sup>28</sup> All  $\text{NaMO}_2$  ternary oxides exhibit such a layered structure as a result of the large difference in size between  $\text{Na}^+$  and  $\text{M}^{3+}$  cation. The reason can readily be explained by examining the symmetry of local atomic coordination structures ( $\text{LiO}_6$ ,  $\text{NaO}_6$ ,  $\text{FeO}_6$  octahedra) for the  $\alpha\text{-NaFeO}_2$  and  $\alpha\text{-LiFeO}_2$  structures.<sup>41</sup> In the  $\alpha\text{-NaFeO}_2$  structure, the Li- or M-centered octahedra are perfect with all Li–O or M–O bond distances being equal. In the  $\alpha\text{-LiFeO}_2$  structure, the Li-centered octahedra are coordinated to four O anions of equal distance from the center, plus two O anions slightly farther away, and the M-centered octahedra are coordinated to two O anions of equal distance from the center, with four more O anions slightly farther away. Atomic relaxation is therefore more efficient in the  $\alpha\text{-NaFeO}_2$  structure because the M–O and Li–O bond distances in the  $\alpha\text{-NaFeO}_2$  structure can relax independently of each other, whereas in the  $\alpha\text{-LiFeO}_2$  structure the relaxation of one set of Li–O or M–O distances will tend to interfere with the relaxation of the other set of Li–O or M–O bond distances (Figure 5). Thus, when the  $\text{Li}^+$  and  $\text{M}^{3+}$  cations are of different sizes, the  $\alpha\text{-NaFeO}_2$  structure is favored because of a more effective relaxation mechanism.

In reality, the 2D order is only observed for  $\text{M} = \text{V}, \text{Cr}, \text{Co}$ , or  $\text{Ni}$ , while for the other 3d cations ( $\text{M} = \text{Ti}, \text{Mn}$ , and  $\text{Fe}$ ), which exhibit a larger ionic radius than those mentioned above, the difference in size in comparison with  $\text{Li}$  is not strong

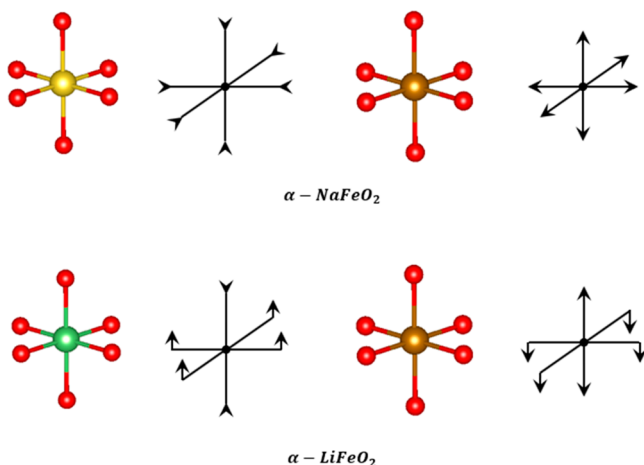


**Figure 5.** Relaxation mechanisms in the  $\alpha\text{-NaFeO}_2$  and  $\alpha\text{-LiFeO}_2$  structures. The yellow, green, brown, and red balls denote Na, Li, Fe, and O, respectively.

enough to induce the 2D order.<sup>28</sup> These results concern only stable materials prepared at high temperature. Though layered  $\text{LiMnO}_2$ <sup>42,43</sup> and rhombohedral  $\text{LiFeO}_2$  ( $R3m$ )<sup>45</sup> can be obtained by exchange from the parent sodium phases, they are metastable and their structure turns into the classical 3D one when heated above 300 °C. This structural classification clearly shows that the driving force of the ordering comes from steric interactions and not from electrostatic ones. Thus, for  $\text{LiCoO}_2$ , the 2D structure is very stable without cationic disorder. For the nickel system, the tendency to order is lowered as a result of the small difference in size between Ni and Li ions.

#### 4.2. Magnetic Interactions

Previous studies including our work found that superexchange interactions exist among transition metals and may provide a new driving force in tuning the Ni/Li disordering.<sup>32,44–46</sup> In the TM layer, due to the unpaired electrons in d orbitals, TM cations will form 90° intraplane superexchanges with neighboring TM cations via a bridged O anion. When Ni/Li exchange happens, the antisite  $\text{Ni}^{2+}$  easily forms interplane 180° (linear) superexchanges with TM cations in the TM layer (Figure 6) via the  $\sigma$  bond formed between the  $e_g$  orbital of the

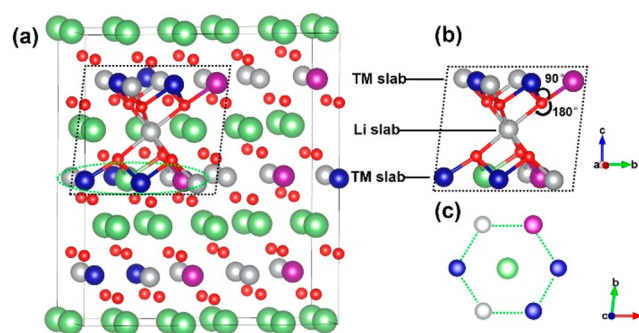


**Figure 6.** (a) The structure model for layered  $\text{LiTMO}_2$  with one pair of Ni/Li exchange. (b) Illustration of the intraplane 90° superexchange interaction between TM cations in the TM layer and the interplane 180° superexchange interaction between the Ni at the Li site and the TM cations in the TM layer. (c) The ion environment of the antisite Li in the TM layer. Adapted with permission from ref 32. Copyright 2017 American Chemical Society.

antisite  $\text{Ni}^{2+}$  and the p orbital of  $\text{O}^{2-}$ . Due to the stronger  $\sigma$  bond, the 180° magnetic interactions are always stronger than the 90° interactions.<sup>38,39</sup> In NMC materials with pure  $\text{Ni}^{2+}$ ,  $\text{Ni}^{2+}$  has the tendency to exchange with Li to form strong linear  $\text{Ni}^{2+}\text{-O}^{2-}\text{-Ni}^{2+}/\text{Mn}^{4+}$  superexchange, while in NMC materials with mixed valence states of  $\text{Ni}^{2+}/\text{Ni}^{3+}$ ,  $\text{Ni}^{3+}$  has the priority to exchange with Li and changes to a  $\text{Ni}^{2+}$  state with a spin-flip, to form strong linear  $\text{Ni}^{2+}\text{-O}^{2-}\text{-Ni}^{2+}/\text{Mn}^{4+}$  superexchanges.<sup>32</sup> Thus, the strong interlayer linear  $\text{Ni}^{2+}\text{-O}^{2-}\text{-Ni}^{2+}/\text{Mn}^{4+}$  superexchange provides an important driving force for Ni/Li exchange. Due to the absence of unpaired electron in the electronic configuration of  $\text{Co}^{3+}$  ( $t_{2g}^6e_g^0$ ), the interlayer linear  $\text{Ni}^{2+}\text{-O}^{2-}\text{-Co}^{3+}$  superexchange with the antisite  $\text{Ni}^{2+}$  is very weak, and the  $\text{Co}^{3+}$  can screen the 180°  $\text{Ni}^{2+}\text{-O}^{2-}\text{-Ni}^{2+}/\text{Mn}^{4+}$  interlayer linear superexchange interactions and thus effectively reduce the concentration of Ni/Li exchange. Adding  $\text{Mn}^{4+}$  has been shown to be effective in improving the thermal stability but may aggravate the  $\text{Ni}^{2+}/\text{Li}^+$  disordering because equivalent amounts of  $\text{Ni}^{2+}$  ions are introduced for charge compensation.<sup>32</sup> Furthermore, by performing neutron powder diffraction

experiments and magnetization measurements, we found the existence of strongly frustrated magnetic interactions between spins of TM ions via the intraplane superexchange interactions within the TM layer<sup>29</sup> (Figure 7). As frustration will inevitably

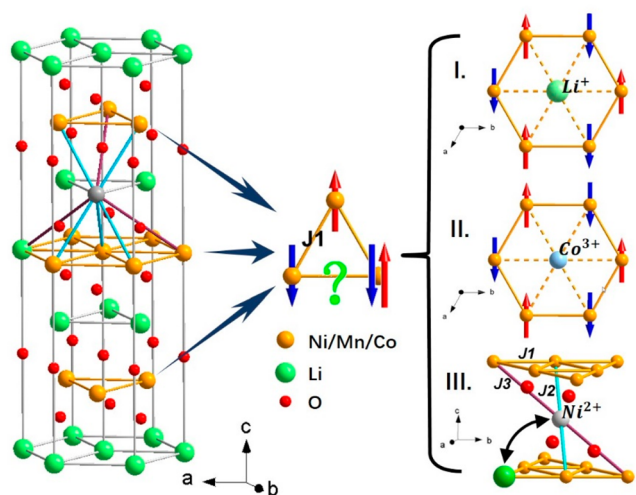


**Figure 7.** Illustration of a pair of Ni/Li exchange and arrangement of magnetic moments in the TM layer of the triangular lattice.  $J_1$  denotes the intraplane superexchange interaction, and  $J_2$  and  $J_3$  denote the interplane superexchange interactions. Adapted with permission from ref 29. Copyright 2018 Elsevier.

give rise to lattice instability,<sup>47</sup> the Ni/Li exchange in NMC will help to partially relieve the degeneracy of the frustrated magnetic lattice by forming a stable antiferromagnetic state in the hexagonal sublattice with nonmagnetic ions ( $\text{Li}^+$ ) located in centers of the hexagons. Moreover, Ni/Li exchange will introduce interlayer linear superexchange interaction, which further relieves the magnetic frustration through bringing in new exchange paths. The addition of nonmagnetic  $\text{Co}^{3+}$  also can act as an ingredient to relieve magnetic frustration by forming a nonmagnetic center on a honeycomb lattice unit so that the surrounding TM spins can be stabilized in an antiferromagnetic arrangement.

### 4.3. Kinetic Advantage

The low energy barrier for the migration of  $\text{Ni}^{2+}$  is also believed to further provide a kinetic advantage for the Ni/Li exchange. Previous theoretical studies show that the energy favorable pathway for Ni migration from the TM layer to Li vacancy in the Li layer is through a nearest neighbor tetrahedral site via the face it shares with the neighboring octahedron (named as  $\text{O}_h\text{-T}_d\text{-O}_h$ ).<sup>48</sup> Using ab initio calculations, Kim et al. reported that the energy barrier for  $\text{Ni}^{2+}$  migration along the  $\text{O}_h\text{-T}_d\text{-O}_h$  path in  $\text{Li}(\text{Ni}_{1-x}\text{Co}_x)\text{O}_2$  is 0.598–0.303 eV during delithiation (from 100% Li to 0% Li),<sup>49</sup> which is comparable to the Li ion migration barriers in NMC materials (Figure 8). By contrast, the Co migration barrier in  $\text{Li}_{0.5}\text{CoO}_2$  is 1.6 eV. The above results also show that the delithiation process (or the Li loss) will facilitate the  $\text{Ni}^{2+}$  migration. In addition, they also found that the O loss (during electrochemical cycling or in high temperature processing) will further promote the  $\text{Ni}^{2+}$  migration from the TM layer to Li layer by providing a new migration pathway of  $\text{O}_h(\text{Ni}) \rightarrow \text{V}_\text{O}$  site  $\rightarrow \text{O}_h(\text{Li})$  ( $\text{V}_\text{O}$  denotes O vacancy), with similar probabilities for Ni migration in the Li 100% and Li 50% configurations to the  $\text{O}_h\text{-T}_d\text{-O}_h$  path (Figure 8). Recently,

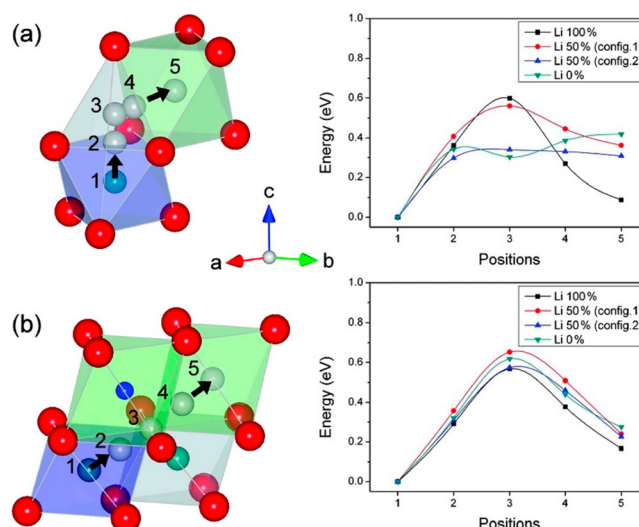


**Figure 8.** Migration routes of Ni ions to Li sites in the layered structure for (a) the  $\text{O}_h \rightarrow \text{T}_d \rightarrow \text{O}_h$  route and (b) the  $\text{O}_h \rightarrow \text{V}_\text{O}$  site  $\rightarrow \text{O}_h$  route and the corresponding energy barriers. Reproduced with permission from ref 49. Copyright 2011 American Chemical Society.

using in situ multimodal synchrotron X-ray techniques, we revealed the dissociation of  $\text{OH}^-$  from  $\text{Ni}(\text{OH})_6$  octahedra leading to asymmetric  $\text{NiO}_{6-x}$  octahedra, and finally the oxidation and symmetry reconstruction of  $\text{NiO}_{6-x}$  octahedra resulting in  $\text{NiO}_6$  octahedra during synthesis of high-Ni NMC materials<sup>50</sup> (Figure 9), which played a crucial role in governing

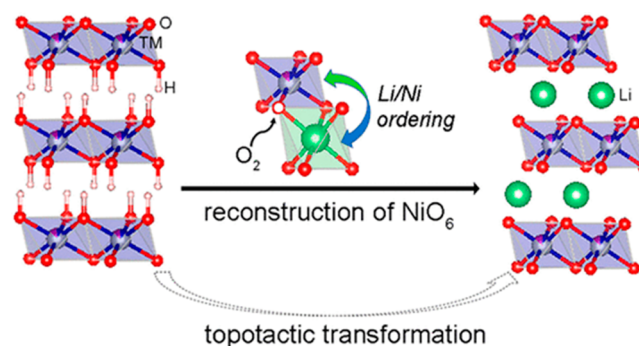


**Figure 9.** Illustration of Ni/Li ordering coupled to reconstruction of  $\text{NiO}_6$  during the topotactic transformation from hydroxides to the layered structure. Adapted with permission from ref 50. Copyright 2018 American Chemical Society.

the reaction pathway and the associated Ni/Li mixing/ordering processes. This can be attributed to the very low activation energy for  $\text{Ni}^{2+}$  migration under the symmetry breaking of  $\text{NiO}_6$  octahedra.

## 5. THE CONTROL OF Ni/LI DISORDERING

Based on above understandings, the methods to control the Ni/Li disordering can be summarized as follows.

### 5.1. Suppressing the Driving Force from the Steric Effect

For the  $\text{AMO}_2$  composition, if the  $\text{A}^+$  ( $\text{A} = \text{alkali metal}$ ) and  $\text{M}^{3+}$  cations are approximately the same size, the Coulombic interactions should dominate and the  $\alpha\text{-LiFeO}_2$  structure will be stable, whereas if the  $\text{A}^+$  and  $\text{M}^{3+}$  cations are of different sizes, atomic relaxations will favor the  $\alpha\text{-NaFeO}_2$  structure. Thus, Kang et al. proposed a method to reduce the degree of

Ni/Li disordering in  $\text{LiNi}_{0.5}\text{Mn}_{0.5}\text{O}_2$  by preparing it via ion exchange from  $\text{NaNi}_{0.5}\text{Mn}_{0.5}\text{O}_2$ .<sup>24</sup>  $\text{NaNi}_{0.5}\text{Mn}_{0.5}\text{O}_2$  exhibits no disorder because of the larger size difference between  $\text{Na}^+$  ( $r_{\text{Na}^+} = 1.02 \text{ \AA}$ ) and  $\text{Ni}^{2+}$  ( $r_{\text{Ni}^{2+}} = 0.69 \text{ \AA}$ ) and  $\text{Mn}^{4+}$  ( $r_{\text{Mn}^{4+}} = 0.53 \text{ \AA}$ ).  $\text{LiNi}_{0.5}\text{Mn}_{0.5}\text{O}_2$  prepared via ion exchange from  $\text{NaNi}_{0.5}\text{Mn}_{0.5}\text{O}_2$  exhibits greatly improved rate capability, delivering  $183 \text{ mAh g}^{-1}$  at a 6C rate.

## 5.2. Cationic Substitution

As we discussed, the addition of Co in layered  $\text{LiTMO}_2$  can reduce the Ni/Li disordering by screening the  $180^\circ \text{ Ni}^{2+} - \text{O}^{2-} - \text{Ni}^{2+}/\text{Mn}^{4+}$  interlayer linear superexchange interactions and relieving magnetic frustration.<sup>32</sup> Other transition metals without unpaired spins at the valence state in layered materials could play the same role as Co. For examples,  $\text{Ti}^{4+}$  and  $\text{Ir}^{3+}$  without unpaired spins would play the same role as Co in layered materials. Actually, the metals that could play the same role as Co can be extended to other nontransition metals, such as  $\text{Al}^{3+}$ , because they also do not have unpaired spins.  $\text{Al}^{3+}$  substituting TM metals would also suppress the Ni/Li exchange, as demonstrated by a previous theoretical study that compared it with  $\text{LiNi}_{1/3}\text{Co}_{1/3}\text{Mn}_{1/3}\text{O}_2$ ; the formation energy of Ni/Li exchange in  $\text{LiNi}_{1/3}\text{Co}_{1/3}\text{Al}_{1/3}\text{O}_2$  is increased from 0.57 to 1.14 eV.<sup>51</sup>

Reducing the content of  $\text{Ni}^{2+}$  can also suppress the Ni/Li disordering, which can be realized by substitution of TM cations with metals of low valence states. Taking the Li-excess layered TM oxides, for example, when part of the TM cations are substituted with  $\text{Li}^+$ , oxidation of a TM ion is needed to maintain the charge neutrality.<sup>52,53</sup> The metal element that is oxidized is the nickel, because the oxidation of  $\text{Ni}^{2+}$  is energetically more favorable than that of  $\text{Mn}^{4+}$  and  $\text{Co}^{3+}$ . Thus, the content of  $\text{Ni}^{2+}$  is reduced, as well as the Ni/Li exchange. It is reported that in  $\text{Li}_{1+x}(\text{NMC})_{1-x}\text{O}_2$  ( $x = 0.02, 0.04$ ), the concentration of  $\text{Ni}^{2+}$  3b ions is lower than 2%.<sup>52</sup>

## 5.3. Tuning the Thermodynamic and Kinetic Conditions and Surface Reactions during Synthesis

As Ni/Li disordering usually happens during the material synthesis procedure, tuning the thermodynamic and kinetic conditions during synthesis is critical to controlling the desired degree of Ni/Li disordering in layered  $\text{LiTMO}_2$ , especially in the presence of high Ni content. Such approaches include tuning the temperature and holding time during heat treatment in the synthesis process.<sup>21,22,27</sup> Using time-resolved in situ high-energy XRD (HEXRD) and X-ray absorption spectroscopy (XAS), Wang et al. by carefully tuning heating temperature and holding time obtained highly ordered  $\text{LiNi}_{0.7}\text{Mn}_{0.15}\text{Co}_{0.15}\text{O}_2$  with excellent electrochemical performance<sup>21</sup> (Figure 10). During the preheating process, oxidation to TMs had already occurred, bringing Co and Mn to the highest oxidation states (i.e.,  $\text{Co}^{3+}$  and  $\text{Mn}^{4+}$ ), and Co and Mn will be first stabilized in the TM layer. When the heat treatment was increased to  $850^\circ\text{C}$ , further oxidation of Ni and structural ordering in the material is triggered. The antisite  $\text{Ni}^{2+}$  in the Li layer is oxidized to  $\text{Ni}^{3+}$ , which will migrate from the 3b site to the 3a site as  $\text{Ni}^{3+}$  favors the 3a site in the TM layer thermodynamically. It should be noted that if the heating temperature is continuously increased to higher values to provide activation energy ( $E_a$ ) for the disordering, the Ni/Li disordering process would be promoted. Moreover, under real synthesis conditions, the serious Li/O loss at higher temperature will also further promote this Ni/Li disordering process by improving the kinetic advantage of  $\text{Ni}^{2+}$  migration from 3a

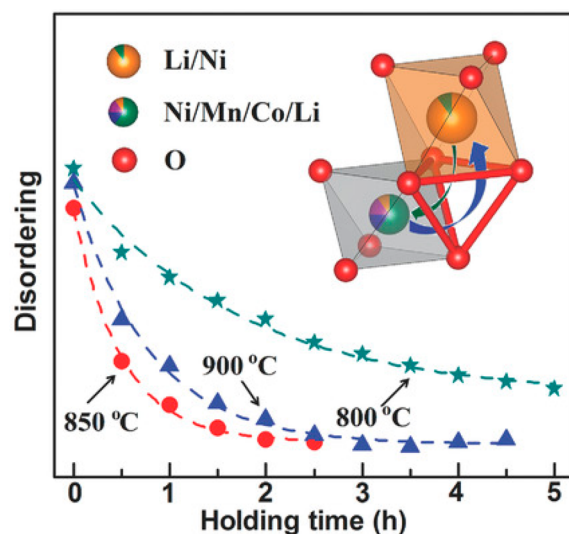


**Figure 10.** Tuning thermodynamic and kinetic parameters to control the Ni/Li ordering in high-Ni layered NMC materials. Adapted with permission from ref 21. Copyright 2017 Wiley.

to 3b sites. Thus, from the view of thermodynamics and kinetics, lower heating temperature and longer holding time is beneficial to the ordering of final products once the temperature is high enough to drive the ordering process. The longer holding time will degrade the kinetics of  $\text{Ni}^{2+}$  migration from the 3a site to 3b site by slowing the Li/O loss during sintering.

Our recent work indicates that surface reactions have significant impacts on the cationic ordering/disordering kinetics in the bulk for Ni-rich NMC.<sup>54</sup> The reaction between atmospheric  $\text{CO}_2$  and the raw material ( $\text{LiOH}$ ) forms  $\text{Li}_2\text{CO}_3$  on the particle surfaces during the synthesis process. Sufficient sintering temperatures are needed to provide enough driving force for the oxidation of antisite  $\text{Ni}^{2+}$  to  $\text{Ni}^{3+}$  as well as  $\text{Li}_2\text{CO}_3$  decomposition, leading to the migration of antisite  $\text{Ni}^{3+}$  back to the TM layer and more Li diffusion from the surface to the bulk to occupy the 3b sites during the synthesis process. Thus, little residual  $\text{LiOH}$  and  $\text{Li}_2\text{CO}_3$  would be formed on the particle surface. Insufficient sintering temperatures would lead to more Ni/Li exchange (more  $\text{Ni}^{2+}$ ) and more residual  $\text{LiOH}$  and  $\text{Li}_2\text{CO}_3$  formed. However, if the sintering temperature is too high, the rate of Li/O loss will be greatly accelerated to promote the Ni/Li exchange.

## 6. CONCLUSIONS AND PERSPECTIVES

Controlling the degree of Ni/Li disordering is an effective way to further improve the performance of layered  $\text{LiTMO}_2$  and has attracted increasing attention. The steric effect of the cations and the interlayer linear superexchange interactions between TM cations and antisite  $\text{Ni}^{2+}$  provide the driving forces to promote the Ni/Li exchange during the synthesis procedure and the electrochemical cycling, and the low energy barrier of  $\text{Ni}^{2+}$  migration from the 3a site in TM layer to 3b site in Li layer further facilitates the Ni/Li exchange kinetically. Moreover, the delithiation (Li loss) and O loss in the lattice of layered  $\text{LiTMO}_2$  would lower the energy barrier for  $\text{Ni}^{2+}$  migration and introduce extra migration pathways to further enhance the kinetic advantage of  $\text{Ni}^{2+}$  migration. Based on current understanding of the formation process of Ni/Li exchange and the related mechanism, feasible ways for

controlling the Ni/Li disordering in layered LiTMO<sub>2</sub> are identified.

It should be noted that as mentioned in the second part, a few studies including our work reported that though the Ni/Li disordering adversely affects diffusion of Li ions, proper content of Ni/Li disordering benefits the thermal stability and the cycling stability of Ni-rich NMC materials. Thus, what degree of the Ni/Li disordering should be balanced to obtain the best electrochemical performance should be clarified in future works for the development of Ni-rich NMC materials.

This Account shows that though the interlayer linear superexchange interactions between TM cations promote the Ni/Li exchange, they can enhance the thermal stability by stabilizing the lattice O ions in Ni-rich NMC materials. In future works, we can find other doping elements to perform the same role as Co to suppress the interlayer linear superexchange interaction to control the Ni/Li disordering, which gives ideas to develop low-cobalt or cobalt-free layered compounds. In addition, finding other elements with large size and unpaired 3d electrons doped at the 3b sites in the Li layer would be interesting, such as Zr<sup>3+</sup> (ref 30). Different from the antisite Ni<sup>2+</sup>, this doped element with large size can increase the Li slab space to facilitate the Li ion diffusion. Moreover, the unpaired 3d electrons of the doped element would also form interlayer linear superexchange interactions with TM cations in the TM layer to stabilize the lattice O, thus benefiting the thermal stability.

Our studies show that cationic ordering is highly coupled to the reconstruction of octahedra upon formation of the layered phase, and due to the high diffusivity of Ni in the symmetry-broken NiO<sub>6</sub> octahedra, serious Ni/Li mixing occurs. Findings from this study highlight the vital importance of tuning the symmetry of NiO<sub>6</sub> octahedra during synthesis of high-Ni layered oxides of high structural ordering. Meanwhile, more experiments should be attempted to find the best the temperature and holding time during heat treatment in the synthesis process, which should balance the thermodynamic and kinetic conditions and surface reactions to control the Ni/Li disordering.

Finally, developing Li-excess layered TM oxides has attracted great interest recently due to the high reversible capability. As we discussed, the Li-excess can suppress the Ni/Li disordering by reducing the Ni<sup>2+</sup> content, so the Li-excess layered TM oxides will not suffer the problem of Ni/Li disordering. The biggest problem of Li-excess layered TM oxides is the O loss during the delithiation process with anionic redox. The antisite Ni<sup>2+</sup> can form strong interlayer linear superexchange interactions with the Mn<sup>4+</sup> in the TM layer to enhance the stability of lattice O. Thus, proper content of antisite Ni<sup>2+</sup> in the Li-layer is also needed to develop Li-excess layered TM oxides.

## AUTHOR INFORMATION

### Corresponding Author

\*E-mail: panfeng@pksuz.edu.cn.

ORCID 

Chongmin Wang: 0000-0003-3327-0958

Feng Wang: 0000-0003-4068-9212

Feng Pan: 0000-0002-8216-1339

### Notes

The authors declare no competing financial interest.

## Biographies

**Jiixin Zheng** received his Ph.D. in Condensed Physics from Peking University in 2013. He is currently working at Peking University as an Associate Professor in the School of Advanced Materials. His research interests include computational materials and energy materials.

**Yaokun Ye** is currently a Ph.D. candidate at Peking University, China. His research interests include computational materials and energy materials.

**Tongchao Liu** is currently a Ph.D. candidate at Peking University, China. His research interests include energy materials, electrochemistry, synchrotron X-ray diffraction, and X-ray absorption spectroscopy.

**Yinguo Xiao** received his Ph.D. degree from Institute of Physics, Chinese Academy of Sciences, China, in 2006. His research interests are on development of new materials for energy conversion and storage and characterization of complex materials using X-ray and neutron scattering techniques.

**Chongmin Wang** is a staff scientist at Environmental Molecular Sciences Laboratory, Pacific Northwest National Laboratory. His research is focused on SEM and TEM, especially in situ SEM and TEM, and energy materials. He is the recipient of MRS Innovation in Materials Characterization Award, JMR Paper of the Year Award, Microscopy Today Innovation Award, Rowland Snow Award, R&D100 Award, Outstanding Invention Award (Japan), and PNNL Directors Award for Exceptional Scientific Achievement.

**Feng Wang** is a materials scientist at the Brookhaven National Laboratory, and a principal investigator leading multiple projects, ranging from basic research on structural characterization to the applied energy storage technologies for transportation and grids. He has 10+ years of research experience in developing advanced electron microscopy and synchrotron X-ray techniques as applied to materials design, synthesis, and characterization.

**Feng Pan** is Chair-Professor, Founding Dean of School of Advanced Materials, Peking University, Shenzhen Graduate School. He received his Ph.D. from the Department of P&A Chemistry, University of Strathclyde, Glasgow, U.K., receiving the "Patrick D. Ritchie Prize" for the best Ph.D. in 1994. Prof. Pan has been engaged in fundamental research and product development of novel optoelectronic and energy storage materials and devices. He was selected as one of the 2018 winners of ECS Battery Division Technology Award.

## ACKNOWLEDGMENTS

This work was financially supported by the National Natural Science Foundation of China (No. 21603007), Soft Science Research Project of Guangdong Province (No. 2017B030301013), and Shenzhen Science and Technology Research Grant (ZDSYS20170728102618). C.W. is supported by the Assistant Secretary for Energy Efficiency and Renewable Energy, Office of Vehicle Technologies, of the U.S. Department of Energy under Contract No. DE-AC02-05CH11231, Subcontract No. 18769 and No. 6951379, under the Advanced Battery Materials Research (BMR) program.

## REFERENCES

- (1) Goodenough, J. B.; Kim, Y. Challenges for rechargeable Li batteries. *Chem. Mater.* **2010**, *22*, 587–603.
- (2) Ellis, B. L.; Lee, K. T.; Nazar, L. F. Positive electrode materials for Li-ion and Li-batteries. *Chem. Mater.* **2010**, *22*, 691–714.
- (3) Liu, W.; Oh, P.; Liu, X.; Lee, M. J.; Cho, W.; Chae, S.; Kim, Y.; Cho, J. Nickel-rich layered lithium transition-metal oxide for high-

energy lithium-ion batteries. *Angew. Chem., Int. Ed.* **2015**, *54*, 4440–4457.

(4) Schipper, F.; Erickson, E. M.; Erk, C.; Shin, J.-Y.; Chesneau, F. F.; Aurbach, D. Recent advances and remaining challenges for lithium ion battery cathodes I. Nickel-Rich,  $\text{LiNi}_x\text{Co}_y\text{Mn}_z\text{O}_2$ . *J. Electrochem. Soc.* **2017**, *164*, A6220–A6228.

(5) Tian, C.; Lin, F.; Doeff, M. M. Electrochemical characteristics of layered transition metal oxide cathode materials for lithium ion batteries: surface, bulk behavior, and thermal properties. *Acc. Chem. Res.* **2018**, *51*, 89–96.

(6) Whittingham, M. S. Lithium batteries and cathode materials. *Chem. Rev.* **2004**, *104*, 4271–4302.

(7) Gao, Y.; Yakovleva, M.; Ebner, W. Novel  $\text{LiNi}_{1-x}\text{Ti}_x/2\text{Mg}_{x/2}\text{O}_2$  compounds as cathode materials for safer lithium-ion batteries. *Electrochem. Solid-State Lett.* **1999**, *1*, 117–119.

(8) Ohzuku, T.; Ueda, A.; Nagayama, M.; Iwakoshi, Y.; Komori, H. Comparative study of  $\text{LiCoO}_2$ ,  $\text{LiNi}_{1/2}\text{Co}_{1/2}\text{O}_2$  and  $\text{LiNiO}_2$  for 4 V secondary lithium cells. *Electrochim. Acta* **1993**, *38*, 1159–1167.

(9) Cho, J.; Kim, G.; Lim, H. S. Effect of preparation methods of  $\text{LiNi}_{1-x}\text{Co}_x\text{O}_2$  cathode materials on their chemical structure and electrode performance. *J. Electrochem. Soc.* **1999**, *146*, 3571–3576.

(10) Mueller-Neuhaus, J.; Dunlap, R.; Dahn, J. Understanding irreversible capacity in  $\text{Li}_x\text{Ni}_{1-y}\text{Fe}_y\text{O}_2$  cathode materials. *J. Electrochem. Soc.* **2000**, *147*, 3598–3605.

(11) Shaju, K.; Subba Rao, G. V.; Chowdari, B. Performance of layered  $\text{Li}(\text{Ni}_{1/3}\text{Co}_{1/3}\text{Mn}_{1/3})\text{O}_2$  as cathode for Li-ion batteries. *Electrochim. Acta* **2002**, *48*, 145–151.

(12) Zhang, X.; Mauger, A.; Lu, Q.; Groult, H.; Perrigaud, L.; Gendron, F.; Julien, C. Synthesis and characterization of  $\text{LiNi}_{1/3}\text{Mn}_{1/3}\text{Co}_{1/3}\text{O}_2$  by wet-chemical method. *Electrochim. Acta* **2010**, *55*, 6440–6449.

(13) Gent, W. E.; Li, Y.; Ahn, S.; Lim, J.; Liu, Y.; Wise, A. M.; Gopal, C. B.; Mueller, D. N.; Davis, R.; Weker, J. N.; Park, J.-H.; Doo, S.-K.; Chueh, W. C. Persistent state-of-charge heterogeneity in relaxed, partially charged  $\text{Li}_{1-x}\text{Ni}_{1/3}\text{Co}_{1/3}\text{Mn}_{1/3}\text{O}_2$  secondary particles. *Adv. Mater.* **2016**, *28*, 6631–6638.

(14) Lu, J.; Chen, Z.; Ma, Z.; Pan, F.; Curtiss, L. A.; Amine, K. The role of nanotechnology in the development of battery materials for electric vehicles. *Nat. Nanotechnol.* **2016**, *11*, 1031.

(15) Nam, K. W.; Bak, S. M.; Hu, E.; Yu, X.; Zhou, Y.; Wang, X.; Wu, L.; Zhu, Y.; Chung, K. Y.; Yang, X. Q. Combining in situ synchrotron X-ray diffraction and absorption techniques with transmission electron microscopy to study the origin of thermal instability in overcharged cathode materials for lithium-ion batteries. *Adv. Funct. Mater.* **2013**, *23*, 1047–1063.

(16) Hwang, S.; Kim, S. M.; Bak, S.-M.; Chung, K. Y.; Chang, W. Investigating the reversibility of structural modifications of  $\text{Li}_x\text{Ni}_y\text{Mn}_z\text{Co}_{1-y-z}\text{O}_2$  cathode materials during Initial charge/discharge, at multiple length scales. *Chem. Mater.* **2015**, *27*, 6044–6052.

(17) Zheng, J.; Liu, T.; Hu, Z.; Wei, Y.; Song, X.; Ren, Y.; Wang, W.; Rao, M.; Lin, Y.; Chen, Z.; et al. Tuning of thermal stability in layered  $\text{Li}(\text{Ni}_x\text{Mn}_y\text{Co}_z)\text{O}_2$ . *J. Am. Chem. Soc.* **2016**, *138*, 13326–13334.

(18) Yan, P.; Nie, A.; Zheng, J.; Zhou, Y.; Lu, D.; Zhang, X.; Xu, R.; Belharouak, I.; Zu, X.; Xiao, J.; et al. Evolution of lattice structure and chemical composition of the surface reconstruction layer in  $\text{Li}_{1.2}\text{Ni}_{0.2}\text{Mn}_{0.6}\text{O}_2$  cathode material for lithium ion batteries. *Nano Lett.* **2015**, *15*, 514–522.

(19) Yan, P. F.; Zheng, J. M.; Lv, D. P.; Wei, Y.; Zheng, J. X.; Wang, Z. G.; Kuppam, S.; Yu, J. G.; Luo, L. L.; Edwards, D.; Olszta, M.; Amine, K.; Liu, J.; Xiao, J.; Pan, F.; Chen, G. Y.; Zhang, J. G.; Wang, C. M. Atomic-resolution visualization of distinctive chemical mixing behavior of Ni, Co, and Mn with Li in layered lithium transition-metal oxide cathode materials. *Chem. Mater.* **2015**, *27*, 5393–5401.

(20) Yu, H.; Qian, Y.; Otani, M.; Tang, D.; Guo, S.; Zhu, Y.; Zhou, H. Study of the lithium/nickel ions exchange in the layered  $\text{LiNi}_{0.42}\text{Mn}_{0.42}\text{Co}_{0.16}\text{O}_2$  cathode material for lithium ion batteries: experimental and first-principles calculations. *Energy Environ. Sci.* **2014**, *7*, 1068–1078.

(21) Wang, D.; Kou, R.; Ren, Y.; Sun, C. J.; Zhao, H.; Zhang, M. J.; Li, Y.; Huq, A.; Ko, J. P.; Pan, F.; et al. Synthetic control of kinetic reaction pathway and cationic ordering in high-Ni layered oxide cathodes. *Adv. Mater.* **2017**, *29*, 1606715.

(22) Zhao, J.; Zhang, W.; Huq, A.; Mixture, S. T.; Zhang, B.; Guo, S.; Wu, L.; Zhu, Y.; Chen, Z.; Amine, K.; et al. In situ probing and synthetic control of cationic ordering in Ni-Rich layered oxide cathodes. *Adv. Energy Mater.* **2017**, *7*, 1601266.

(23) Sun, Y.-K.; Lee, D.-J.; Lee, Y. J.; Chen, Z.; Myung, S.-T. Cobalt-free nickel rich layered oxide cathodes for lithium-ion batteries. *ACS Appl. Mater. Interfaces* **2013**, *5*, 11434–11440.

(24) Kang, K.; Meng, Y. S.; Bréger, J.; Grey, C. P.; Ceder, G. Electrodes with high power and high capacity for rechargeable lithium batteries. *Science* **2006**, *311*, 977–980.

(25) Bréger, J.; Dupré, N.; Chupas, P. J.; Lee, P. L.; Proffen, T.; Parise, J. B.; Grey, C. P. Short-and long-range order in the positive electrode material,  $\text{Li}(\text{NiMn})_{0.5}\text{O}_2$ : A joint X-ray and neutron diffraction, pair distribution function analysis and NMR study. *J. Am. Chem. Soc.* **2005**, *127*, 7529–7537.

(26) Meng, Y.; Ceder, G.; Grey, C.; Yoon, W.-S.; Jiang, M.; Breger, J.; Shao-Horn, Y. Cation Ordering in Layered  $\text{O}_3$   $\text{Li}[\text{Ni}_x\text{Li}_{1/3-2x/3}\text{Mn}_{2/3-x/3}]\text{O}_2$  ( $0 \leq x \leq 1/2$ ) Compounds. *Chem. Mater.* **2005**, *17*, 2386–2394.

(27) Sun, G.; Yin, X.; Yang, W.; Song, A.; Jia, C.; Yang, W.; Du, Q.; Ma, Z.; Shao, G. The effect of cation mixing controlled by thermal treatment duration on the electrochemical stability of lithium transition-metal oxides. *Phys. Chem. Chem. Phys.* **2017**, *19*, 29886–29894.

(28) Rougier, A.; Saadoun, I.; Gravereau, P.; Willmann, P.; Delmas, C. Effect of cobalt substitution on cationic distribution in  $\text{LiNi}_{1-y}\text{Co}_y\text{O}_2$  electrode materials. *Solid State Ionics* **1996**, *90*, 83–90.

(29) Xiao, Y.; Liu, T.; Liu, J.; He, L.; Chen, J.; Zhang, J.; Luo, P.; Lu, H.; Wang, R.; Zhu, W.; et al. Insight into the origin of lithium/nickel ions exchange in layered  $\text{Li}(\text{Ni}_x\text{Mn}_y\text{Co}_z)\text{O}_2$  cathode materials. *Nano Exchange* **2018**, *49*, 77–85.

(30) Yoon, C. S.; Choi, M.-J.; Jun, D.-W.; Zhang, Q.; Kaghazchi, P.; Kim, K.-H.; Sun, Y.-K. Cation ordering of Zr-doped  $\text{LiNiO}_2$  cathode for lithium-ion batteries. *Chem. Mater.* **2018**, *30*, 1808–1814.

(31) Wei, Y.; Zheng, J.; Cui, S.; Song, X.; Su, Y.; Deng, W.; Wu, Z.; Wang, X.; Wang, W.; Rao, M.; et al. Kinetics tuning of Li-ion diffusion in layered  $\text{Li}(\text{Ni}_x\text{Mn}_y\text{Co}_z)\text{O}_2$ . *J. Am. Chem. Soc.* **2015**, *137*, 8364–8367.

(32) Zheng, J.; Teng, G.; Xin, C.; Zhuo, Z.; Liu, J.; Li, Q.; Hu, Z.; Xu, M.; Yan, S.; Yang, W.; Pan, F. Role of superexchange interaction on tuning of Ni/Li disordering in layered  $\text{Li}(\text{Ni}_x\text{Mn}_y\text{Co}_z)\text{O}_2$ . *J. Phys. Chem. Lett.* **2017**, *8*, 5537–5542.

(33) Kang, K.; Ceder, G. Factors that affect Li mobility in layered lithium transition metal oxides. *Phys. Rev. B: Condens. Matter Mater. Phys.* **2006**, *74*, No. 094105.

(34) Delmas, C.; Peres, J.; Rougier, A.; Demourgues, A.; Weill, F.; Chadwick, A.; Broussely, M.; Pertion, F.; Biensan, P.; Willmann, P. On the behavior of the  $\text{Li}_x\text{NiO}_2$  system: an electrochemical and structural overview. *J. Power Sources* **1997**, *68*, 120–125.

(35) Peres, J.; Delmas, C.; Rougier, A.; Broussely, M.; Pertion, F.; Biensan, P.; Willmann, P. The relationship between the composition of lithium nickel oxide and the loss of reversibility during the first cycle. *J. Phys. Chem. Solids* **1996**, *57*, 1057–1060.

(36) Yang, X.-Q.; McBreen, J.; Yoon, W.-S.; Grey, C. P. Crystal structure changes of  $\text{LiMn}_{0.5}\text{Ni}_{0.5}\text{O}_2$  cathode materials during charge and discharge studied by synchrotron based in situ XRD. *Electrochem. Commun.* **2002**, *4*, 649–654.

(37) Chen, Z.; Wang, J.; Chao, D.; Baikie, T.; Bai, L.; Chen, S.; Zhao, Y.; Sum, T. C.; Lin, J.; Shen, Z. Hierarchical porous  $\text{LiNi}_{1/3}\text{Co}_{1/3}\text{Mn}_{1/3}\text{O}_2$  nano-/micro spherical cathode material: Minimized cation mixing and improved  $\text{Li}^+$  mobility for enhanced electrochemical performance. *Sci. Rep.* **2016**, *6*, 25771.

(38) Goodenough, J. B. *Magnetism and the Chemical Bond*; Interscience: New York, 1963.

(39) Kanamori, J. Superexchange interaction and symmetry properties of electron orbitals. *J. Phys. Chem. Solids* **1959**, *10*, 87–98.

(40) Hausbrand, R.; Cherkashinin, G.; Ehrenberg, H.; Grötting, M.; Albe, K.; Hess, C.; Jaegermann, W. Fundamental degradation mechanisms of layered oxide Li-ion battery cathode materials: Methodology, insights and novel approaches. *Mater. Sci. Eng., B* **2015**, *192*, 3–25.

(41) Wu, E. J.; Tepesch, P. D.; Ceder, G. Size and charge effects on the structural stability of  $\text{LiMO}_2$  (M= transition metal) compounds. *Philos. Mag. B* **1998**, *77*, 1039–1047.

(42) Capitaine, F.; Gravereau, P.; Delmas, C. A new variety of  $\text{LiMnO}_2$  with a layered structure. *Solid State Ionics* **1996**, *89*, 197–202.

(43) Fuchs, B.; Kemmler-Sack, S. Synthesis of  $\text{LiMnO}_2$  and  $\text{LiFeO}_2$  in molten Li halides. *Solid State Ionics* **1994**, *68*, 279–285.

(44) Chen, H.; Dawson, J. A.; Harding, J. H. Effects of cationic substitution on structural defects in layered cathode materials  $\text{LiNiO}_2$ . *J. Mater. Chem. A* **2014**, *2*, 7988–7996.

(45) Chernova, N. A.; Ma, M.; Xiao, J.; Whittingham, M. S.; Breger, J.; Grey, C. P. Layered  $\text{Li}_x\text{Ni}_y\text{Mn}_z\text{Co}_{1-2y}\text{O}_2$  cathodes for lithium ion batteries: understanding local structure via magnetic properties. *Chem. Mater.* **2007**, *19*, 4682–4693.

(46) Hinuma, Y.; Meng, Y. S.; Kang, K.; Ceder, G. Phase transitions in the  $\text{LiNi}_{0.5}\text{Mn}_{0.5}\text{O}_2$  system with temperature. *Chem. Mater.* **2007**, *19*, 1790–1800.

(47) Wannier, G. Antiferromagnetism. the triangular ising net. *Phys. Rev.* **1950**, *79*, 357.

(48) Ma, X.; Kang, K.; Ceder, G.; Meng, Y. S. Synthesis and electrochemical properties of layered  $\text{LiNi}_{2/3}\text{Sb}_{1/3}\text{O}_2$ . *J. Power Sources* **2007**, *173*, 550–555.

(49) Kim, Y.; Kim, D.; Kang, S. Experimental and first-principles thermodynamic study of the formation and effects of vacancies in layered lithium nickel cobalt oxides. *Chem. Mater.* **2011**, *23*, 5388–5397.

(50) Zhang, M.-J.; Teng, G.; Chen-Wiegart, Y.-c. K.; Duan, Y.; Ko, J. Y. P.; Zheng, J.; Thieme, J.; Dooryhee, E.; Chen, Z.; Bai, J.; et al. Cationic ordering coupled to reconstruction of basic building units during synthesis of high-Ni layered oxides. *J. Am. Chem. Soc.* **2018**, *140*, 12484–12492.

(51) Hoang, K.; Johannes, M. Defect physics and chemistry in layered mixed transition metal oxide cathode materials: (Ni, Co, Mn) vs (Ni, Co, Al). *Chem. Mater.* **2016**, *28*, 1325–1334.

(52) Zhang, X.; Jiang, W. J.; Mauger, A.; Qilu, Gendron, F.; Julien, C. M. Minimization of the cation mixing in  $\text{Li}_{1+x}(\text{NMC})_{1-x}\text{O}_2$  as cathode material. *J. Power Sources* **2010**, *195*, 1292–1301.

(53) Myung, S.-T.; Komaba, S.; Kurihara, K.; Hosoya, K.; Kumagai, N.; Sun, Y.-K.; Nakai, I.; Yonemura, M.; Kamiyama, T. Synthesis of  $\text{Li}[(\text{Ni}_{0.5}\text{Mn}_{0.5})_{1-x}\text{Li}_x]\text{O}_2$  by emulsion drying method and impact of excess Li on structural and electrochemical properties. *Chem. Mater.* **2006**, *18*, 1658–1666.

(54) Duan, Y.; Yang, L.; Zhang, M.-J.; Chen, Z.; Bai, J.; Amine, K.; Pan, F.; Wang, F. Insights into Li/Ni ordering and surface reconstruction during synthesis of Ni-rich layered oxides. *J. Mater. Chem. A* **2019**, *7*, 513–519.